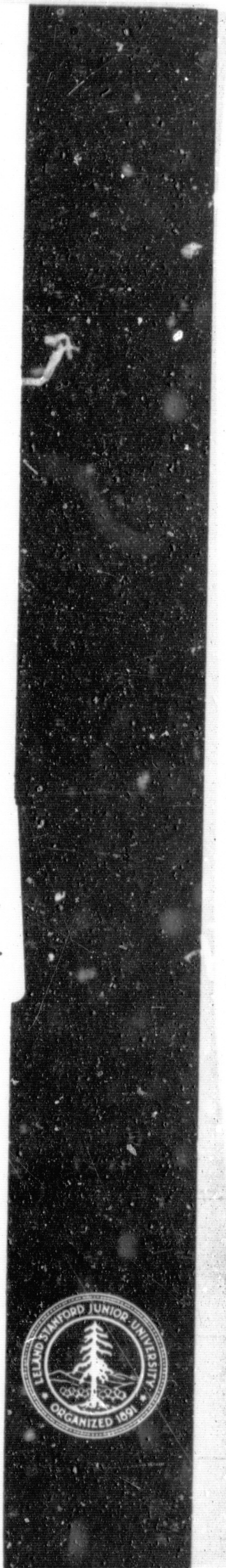

SU-SEL-69-003

The Atmosphere of Venus as Studied with the Mariner 5 Dual Radio-Frequency Occultation Experiment

by

G Fjeldbo and V. R. Eshleman

January 1969

FINAL REPORT, Part I

on Project 3226 and on National Aeronautics and Space Administration Grant NGR 05-020-276

RADIOSCIENCE LABORATORY

STANFORD ELECTRONICS LABORATORIES

STANFORD UNIVERSITY · STANFORD, CALIFORNIA

SEL-69-003

THE ATMOSPHERE OF VENUS AS STUDIED WITH THE MARINER 5 DUAL RADIO-FREQUENCY OCCULTATION EXPERIMENT

by

G. Fjeldbo and V. R. Eshleman

January 1969

FINAL REPORT, Part I

on

Project 3226 and on

National Aeronautics and Space Administration

Grant NGR 05-020-276

Radioscience Laboratory

Stanford Electronics Laboratories

Stanford University Stanford, California

ABSTRACT

The amplitudes and differential doppler of two radio signals transmitted to Mariner 5 as it was occulted by Venus are utilized to derive the day- and night-side ionization distributions in the upper atmosphere and the temperature and pressure profiles of the lower atmosphere. Both sides of Venus have ionization peaks near the 140-km altitude level; the daytime peak is 30 times greater in electron number density. The night-side ionosphere extended up to an altitude of at least 1000 km, and the day-side ionization terminated in a plasmapause near a 500-km altitude. The neutral atmosphere was probed down to within 35 km of the planetary surface.

CONTENTS

ILLUSTRATIONS

ACKNOWLEDGMENTS

Stimulating discussions with B. C. Fair, H. T. Howard, and R. A. Long are gratefully acknowledged. The electron content of the terrestrial ionosphere (Fig. 3) was supplied by H. T. Howard and R. P. Merritt. The Mariner 5 trajectory coordinates were provided by the Systems Analysis Research Section of the Jet Propulsion Laboratory, Pasadena, California.

This research was supported by NASA Grant NGR 05-020-276.

Chapter I

INTRODUCTION

The initial analysis of the Mariner 5 dual RF occultation experiment provided preliminary results for the day and night-side ionization profiles on Venus [Mariner Stanford Group, 1967]. The results were based primarily on integral inversion of the dispersive doppler data, assuming that the effects of multipath propagation were negligible. The purpose of this report is to present the results of a complete study on both the doppler and amplitude data. Model-fitting and inversion techniques are employed, and in addition to deriving ionospheric electron number-density profiles, pressure and temperature profiles for the lower neutral atmosphere are also deduced.

Before describing the analysis of the data, the measurements will be reviewed briefly. The experiment was conducted by transmitting two harmonically related frequencies--49.8 and 423.3 MHz (phase modulated at 7692 or 8692 Hz)--from a 150-ft parabolic dish at Stanford, California, and by receiving the signals with phase-locked receivers in the spacecraft. The transmitter powers were approximately 350 kW at the lower frequency and 30 kW at the higher frequency. Circularly polarized waves were transmitted from the dish, and linearly polarized low-gain antennas were utilized for reception.

The primary purpose of the experiment was to measure the differential doppler and the group path together with signal amplitudes as the spacecraft passed behind the ionosphere and neutral atmosphere of Venus. The data were stored on a tape recorder in the spacecraft and sent back to Earth over the telemetry system after emersion from occultation.

Differential doppler measurements were made by continuously counting the zero crossings of a beat note obtained by comparing the lower frequency to the 2/17 subharmonic of the higher frequency. The doppler counter was read out every 0.6 s during the experiment. The relative phase of the audio-modulation tones of the two radio-frequency carriers provided data on the differential group path. The signal intensities were measured every 0.6 s by sampling the outputs of the amplitude phase detectors.

A more detailed description of the spacecraft's instrumentation has been presented by Long and Fair (1968).

The Mariner 5 occultation measurements were made on 19 October 1967, and Fig. 1 shows the geometry of the experiment. Immersion and emersion occurred on the night and day sides, respectively. A map of Venus illustrating the locations where the atmosphere was probed by the radio signals is shown in Fig. 2. The following chapters summarize the analysis of the data.

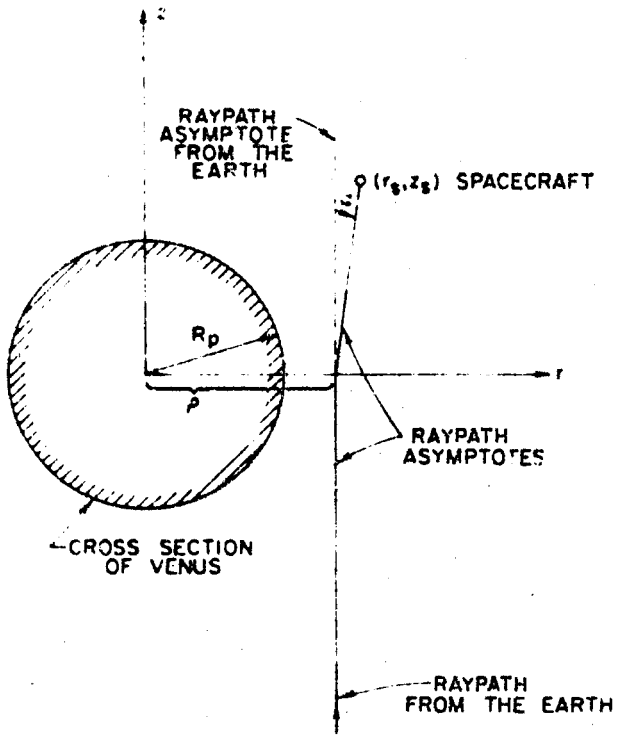

Fig. 1. OCCULTATION GEOMETRY.

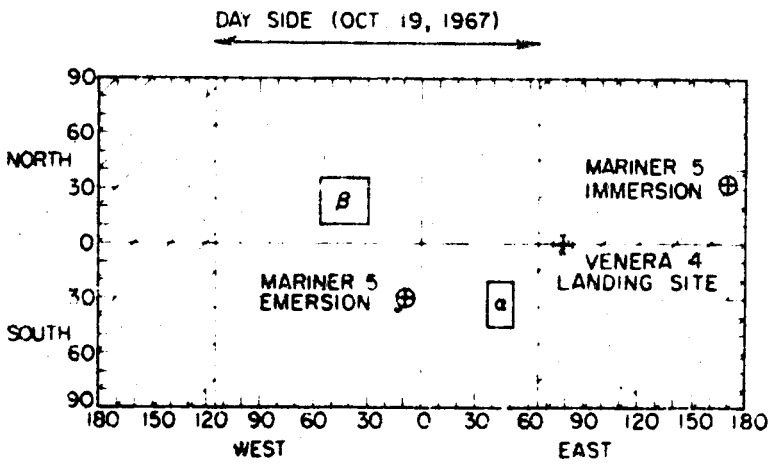

Fig. 2. MAP OF VENUS SHOWING LOCATIONS WHERE OCCULTATION MEASUREMENTS WERE MADE. Zero-meridian plane contains the Earth at inferior conjunction. Areas marked α and β are strong radar scatterers [Goldstein, 1965].

Chapter II

THE PLASMA TAIL

The differential doppler and group-path measurements provide data on the total electron content (integrated electron number density along the propagation path) between Stanford and Mariner 5, and the results obtained near planetary encounter are illustrated in Fig. 3. To utilize these data so as to determine the spatial distribution of free electrons around Venus, the electron content contributed by the rest of the medium (the terrestrial ionosphere and interplanetary space) must be subtracted. The electron content of the Earth's ionosphere was measured between the Applications Technology Satellite (ATS) and Stanford during the experiment, and these results are also shown in Fig. 3, after correcting the ATS measurements for the different path to Mariner. By subtracting the electron content of the Earth's ionosphere from the total content and fitting a straight line to the resulting curve in the time intervals just preceding and following the occultation, it was determined that the average interplanetary electron number density along the path was about 5.06 cm^{-3} at encounter. The corresponding rate of change in this number density was approximately 0.4 cm^{-3} hr^{-1}. With this linear approximation for the interplanetary density, the residual electron content produced by the local ionization surrounding Venus can be computed, and the resulting curve is illustrated in Fig. 4. The rapid changes at -4 and 24 min from encounter were produced by the topside of the night- and day-side ionospheres respectively. The slower increase, commencing approximately 14 min before encounter, may have been caused by a tail (or wake) of ionization extending out on the dark side of Venus, or it could have been produced by a 1.3-percent nonlinear increase in the average interplanetary electron number density at that time.

The linear fit used to approximate the average electron number-density changes in the interplanetary medium is only adequate near occultation. The inclusion of higher order terms would provide a better fit over a larger time interval (and thereby, for example, reduce the residual electron content prior to -26 min) but would not have an important impact on

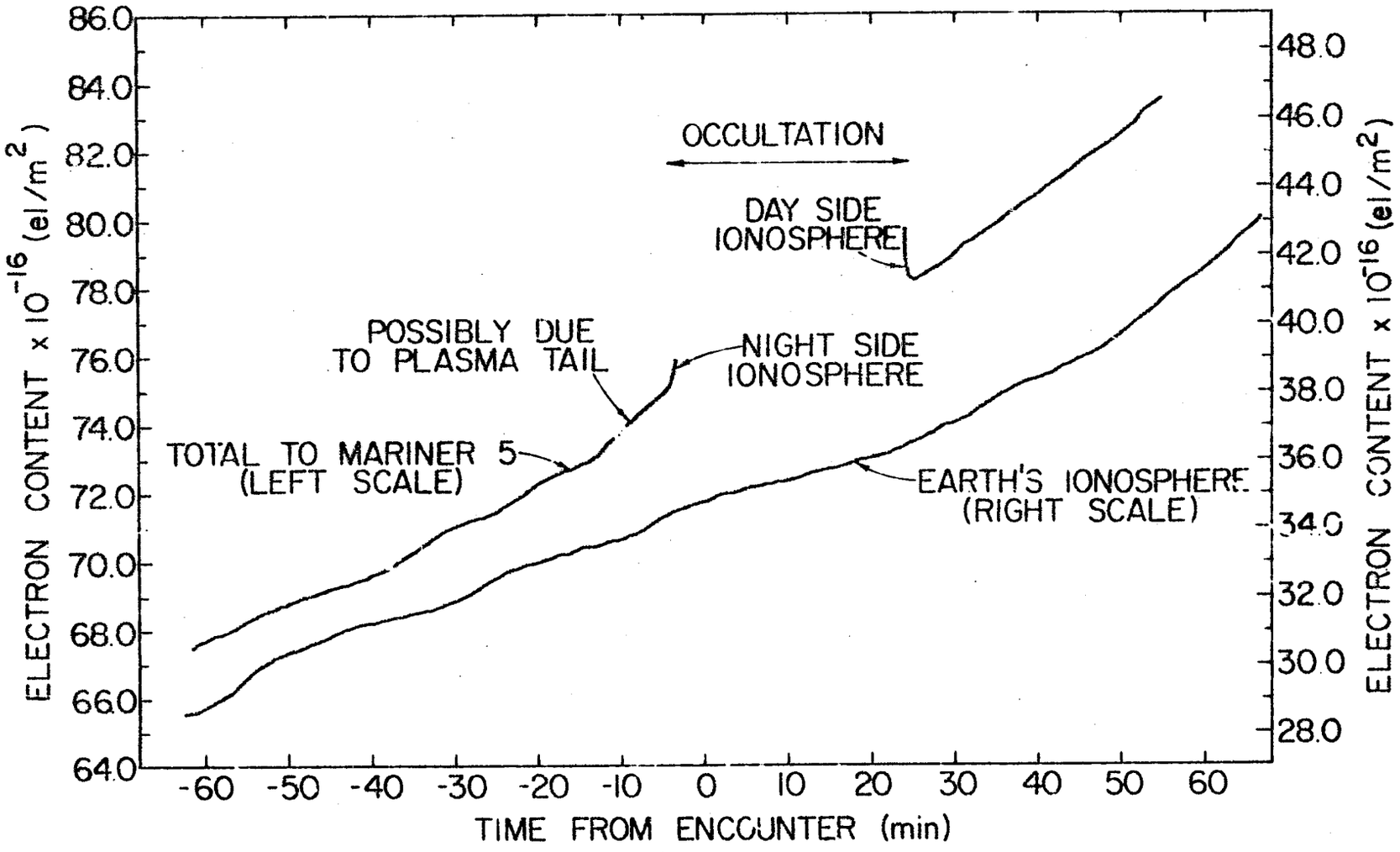

Fig. 3. TOTAL ELECTRON CONTENT ALONG THE PROPAGATION PATH FROM STANFORD TO MARINER 5, AND CONTRIBUTION BY THE FARTH'S IONOSPHERE VS TIME FROM ENCOUNTER (PERIAPSIS).

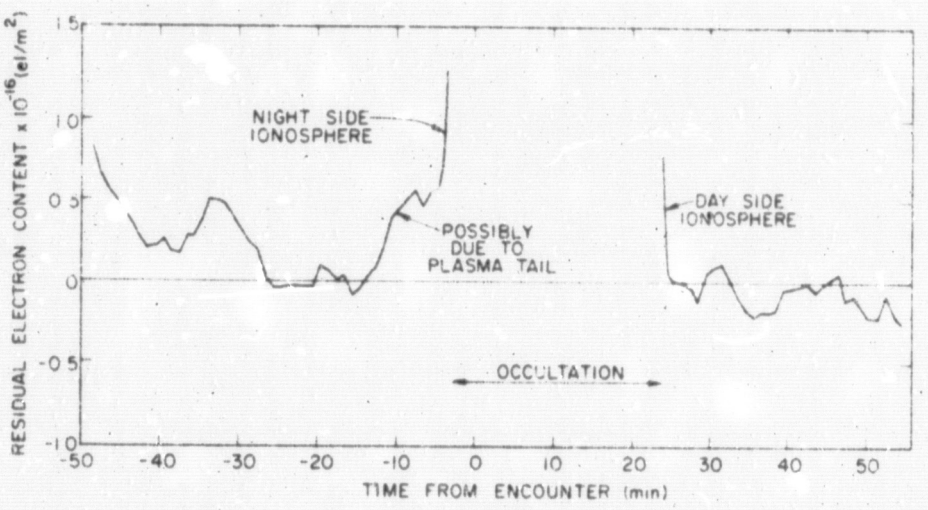

Fig. 4. RESIDUAL ELECTRON CONTENT VS TIME FROM ENCOUNTER. Residual content was obtained by subtracting the contribution from the terrestrial ionosphere and the interplanetary medium from the total content measured between Stanford and Mariner 5. Average interplanetary electron number density at encounter ($5.06\ cm^{-3}$) and its time rate of change ($0.4\ cm^{-3}\ hr^{-1}$) were determined by assuming a zero-mean residual content during time intervals -26 to -14 min and 25 to 33 min.

the question of whether the plasma tail on the night side of Venus is real. The following discussion of the spatial properties of the plasma tail is based on the simple linear approximation to the interplanetary electron number density.

Preliminary analysis of the differential doppler data pertaining to the high-altitude nighttime ionization on Venus was based on the assumption that spherical symmetry prevailed out to at least the 4000-km altitude [Mariner Stanford Group, 1967]. However, the striking differences between the day- and night-side residual electron content data show clearly that the distribution of ionization was not spherically symmetric. Figures 5 and 6 illustrate alternate interpretations based on the assumption that interaction between the solar wind and the upper atmosphere produces an ionization tail predominantly cylindrical in shape with its axis of symmetry parallel to the solar-wind velocity.

A unique determination of the spatial electron number-density distribution in the plasma tail would require occultation measurements along many different paths. To invert the integral equation that relates the electron number density to the residual content of Fig. 4, the density

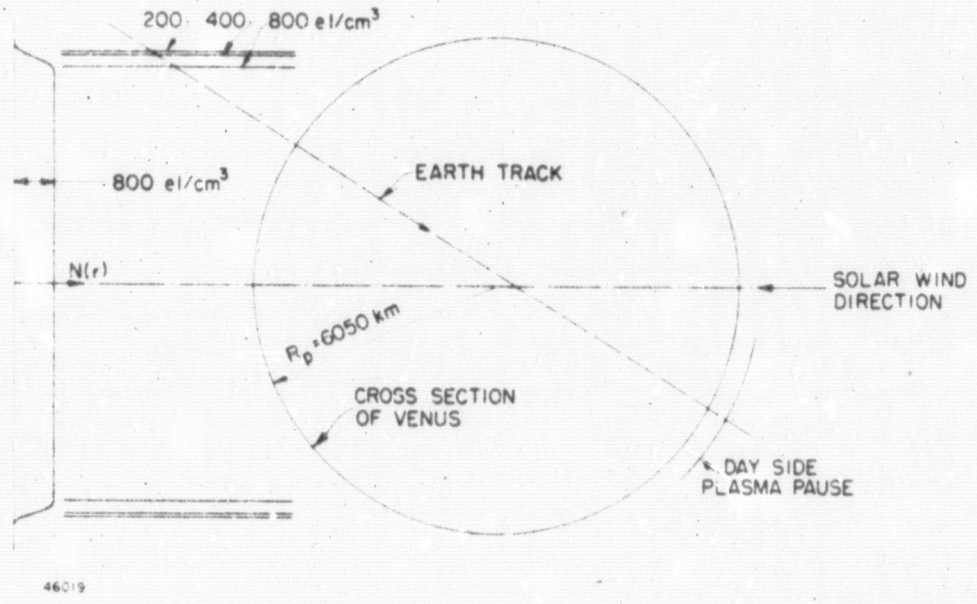

Fig. 5. SPATIAL PLASMA DISTRIBUTION IN TAIL, ASSUMING NO AXIAL NUMBER-DENSITY GRADIENTS. The plane of the figure is perpendicular to the ecliptic. Solar-wind velocity was approximately 575 km/s, corresponding to an aberration angle of 3.5° [Bridge et al, 1967].

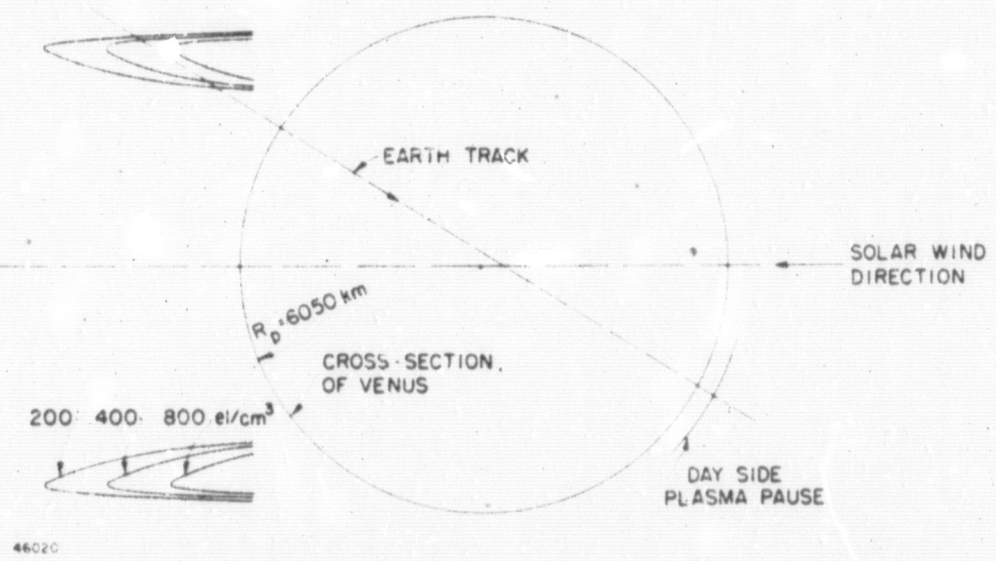

Fig. 6. SPATIAL PLASMA DISTRIBUTION IN TAIL, ASSUMING EXPONENTIAL DECREASE [$\exp(-z/H_z)$] OF THE NUMBER DENSITY ALONG AXIS OF SYMMETRY. H_z = 2250 km.

changes in the axial direction were specified. The corresponding radial variations in the number density then could be calculated readily by adopting techniques described previously [Fjeldbo and Eshleman, 1968]. The results shown in Figs. 5 and 6 are for the cases of no density change and exponential density change, respectively, along the axis of symmetry. These figures illustrate how the number-density distribution changes

when the scale height along the axis of symmetry H_z is increased from 2250 km to infinity. Reducing H_z below 2250 km yields negative values for the number density at a distance of about 4000 km from the axis of the cylinder.

In deriving the residual content of Fig. 4, the ATS data were used to subtract the contribution of the terrestrial ionosphere from the total content. The residual content has also been determined from the Mariner data in a more direct manner, without first separating the content of the interplanetary medium and the terrestrial ionosphere. This computation was done by fitting a straight line to the total electron content (Fig. 3) prior to -13 min and by using this as a zero reference for calculating the residual content. This approach produced essentially the same ionization profiles as those illustrated in Figs. 5 and 6 and shows that what here has been interpreted as ionization on the night side of Venus was not caused by a local anomalous decrease in the terrestrial content along the Stanford-ATS path.

The question of whether the high-altitude residual-content data should be interpreted as an ionization tail is not likely to be resolved before measurements can be repeated with a planetary orbiter. This experimental configuration offers the advantage that the content data can be averaged over many occultations, thereby reducing noise caused by the terrestrial ionosphere and the interplanetary medium. Repeated measurements through different portions of the ionization tail would also provide three-dimensional number-density resolution (if temporal changes are negligible) and, therefore, eliminate the necessity for simplifying assumptions such as those employed in this study.

An even better arrangement would be obtained by simultaneously conducting propagation experiments between the Earth and two orbiters. While one is being used to probe the upper atmosphere, the other could monitor changes in the terrestrial ionosphere and the interplanetary medium and thereby provide zero reference for the residual content. An experiment of this type is planned for the 1971 dual-orbiter mission to Mars. That experiment may also throw new light on the Mariner 5 high-altitude dual-frequency occultation data because both Mars and Venus appear to lack a significant intrinsic magnetic field and, therefore are expected to interact with the solar wind in similar ways.

Chapter III

THE NIGHT-SIDE IONOSPHERE

The principal ionosphere of Venus produces a much larger time rate of change in the electron content than is evident in other portions of the data (see Fig. 3). Interpretation of this feature in the data is therefore affected much less by the electron content noise of terrestrial and interplanetary origin than is the interpretation of the data on the distribution in the tail.

Figure 7 shows the vertical ionization profile on the night side of Venus, assuming that the plasma tail has the form shown in Fig. 5.

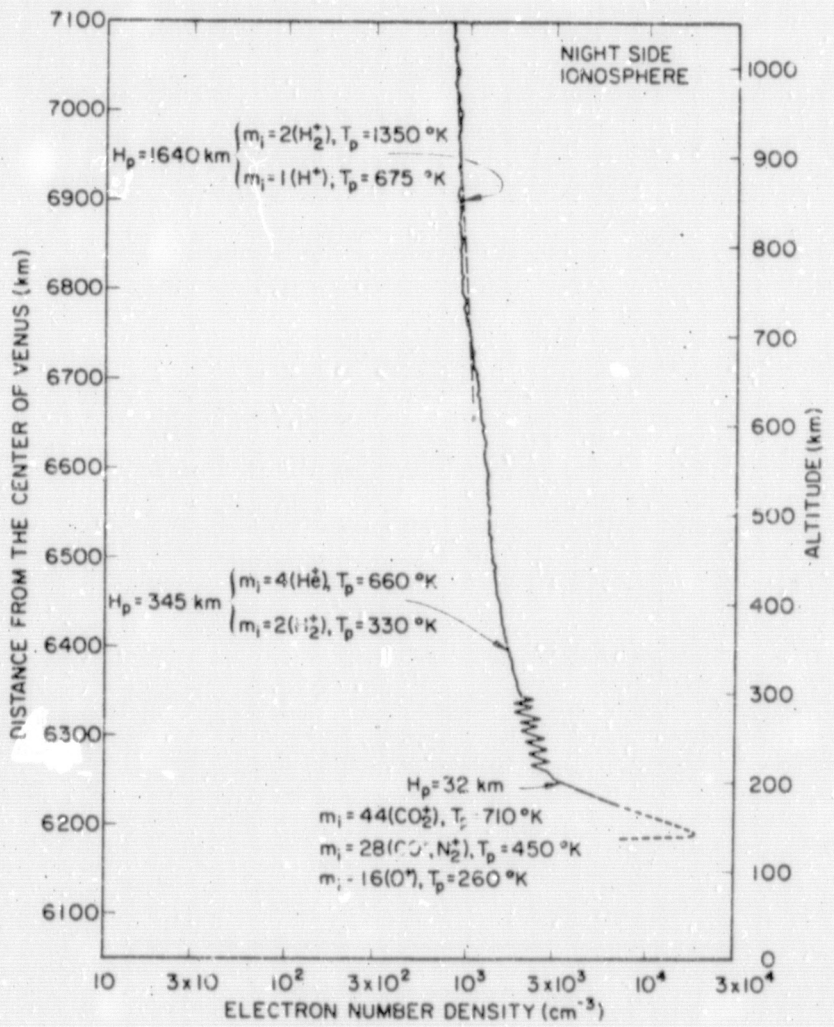

Fig. 7. NIGHT-SIDE IONIZATION PROFILE. Plasma tail was assumed to have the shape shown in Fig. 5.

The solid portion of the curve was obtained by inverting the differential doppler data, assuming spherical symmetry around the planet's center of mass. Running point averages taken over an altitude interval of about 90 km was employed in smoothing the profile above the 300-km altitude.* The noise seen below this level was caused by the doppler count quantization.

Because of the multipath propagation at 49.8 MHz, inversion of the doppler data does not yield an accurate profile in the lower ionosphere. The stippled portion of the profile was therefore deduced from the amplitude variations observed on the 423.3-MHz signal.

The ionization peak near the 142-km altitude has an electron number density of approximately 2×10^{4} cm^{-3}; it is located at the same altitude as the day-side peak and may have been produced by plasma transport from the sunlit side of the planet. It is also possible that the nighttime layer is analogous to the terrestrial E and D regions.

Above the ionization peak, the plasma scale height is approximately 32 km--corresponding to a temperature of 710°K if CO_2^+ is the principal ion. A marked change in the scale height near the 200-km altitude probably reflects the transition to a lighter ion such as He^+; above the 700-km altitude, the principal ion may be H^+. If these interpretations are applicable, all three altitude regimes would have approximately the same plasma temperature, i.e., 660 to 710°K. This temperature is, incidentally, in good agreement with the 650°K day-side thermospheric temperature derived from the Mariner 5 Lyman Alpha measurements [Barth, 1968] and also with theoretical temperature estimates based on a pure CO_2 atmosphere [McElroy, 1968]. A few alternative interpretations, in terms of ion masses and plasma temperatures, are indicated on Fig. 7.

The shape of the ionization profile above the 200-km altitude is very sensitive to how the plasma is distributed in the tail. Figure 8 shows the vertical ionization profile if the plasma tail had the form

---

*The altitude scale utilized in the figures of this report was obtained by assuming a planetary radius of 6050 km. Analyses of radar data [Ash et al, 1968; Melbourne et al, 1968] and work on both radar and Mariner 5 data [Eshleman et al, 1968] yield values for the radius of Venus ranging from 6050 to 6056 km.

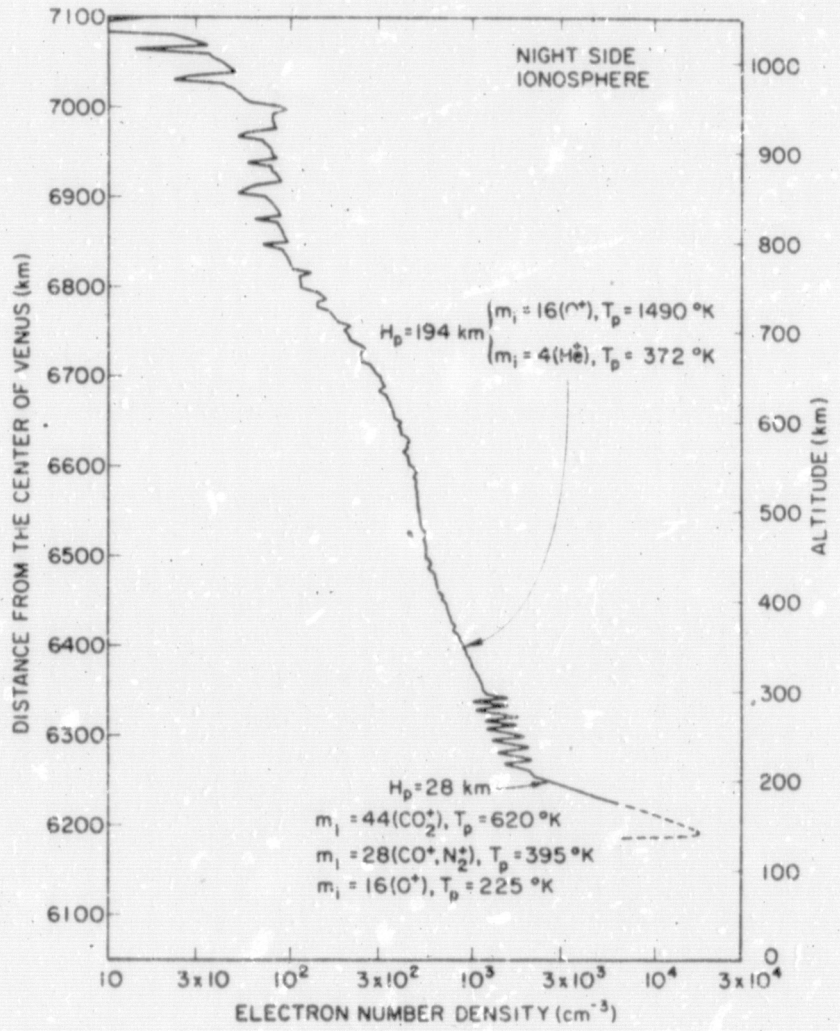

Fig. 8. NIGHT-SIDE IONIZATION PROFILE FOR THE CASE OF NO TAIL. Same result is obtained if plasma tail has the form shown in Fig. 6.

illustrated in Fig. 6; the same profile is obtained for the case of no tail (i.e., if the residual electron content attributed to the tail was caused instead by a nonlinear variation in the interplanetary content).

As already noted, the ionization region near the peak was studied by fitting the defocusing produced by a Chapman layer to the amplitude variations observed on the 423.3-MHz radio link. Four parameters were varied in the Chapman layer: altitude, peak density, and the bottom and topside scale heights. The resulting fit is illustrated in Fig. 9, where the full-drawn and the stippled curves represent the measured and computed signal amplitudes, respectively. The signature of the main layer was observed betweer 3.4 and 3.26 min before encounter. Maximum defocusing occurred at -3.3 min, when the radio ray passed 4 km (about half the bottomside scale height) below the ionization peak. At 3.18 min

to encounter, the amplitude started dropping sharply because of defocusing in the lower neutral atmosphere.

Figure 9 shows that the signal level on the 423.3-MHz channel fluctuated about ±1 dB, with a period of the order of 1 s during the time interval from -3.26 to -3.18 min from encounter; however, the period of these oscillations may actually have been shorter than 1 s. This cannot be verified because the spacecraft instrument only sampled the amplitude

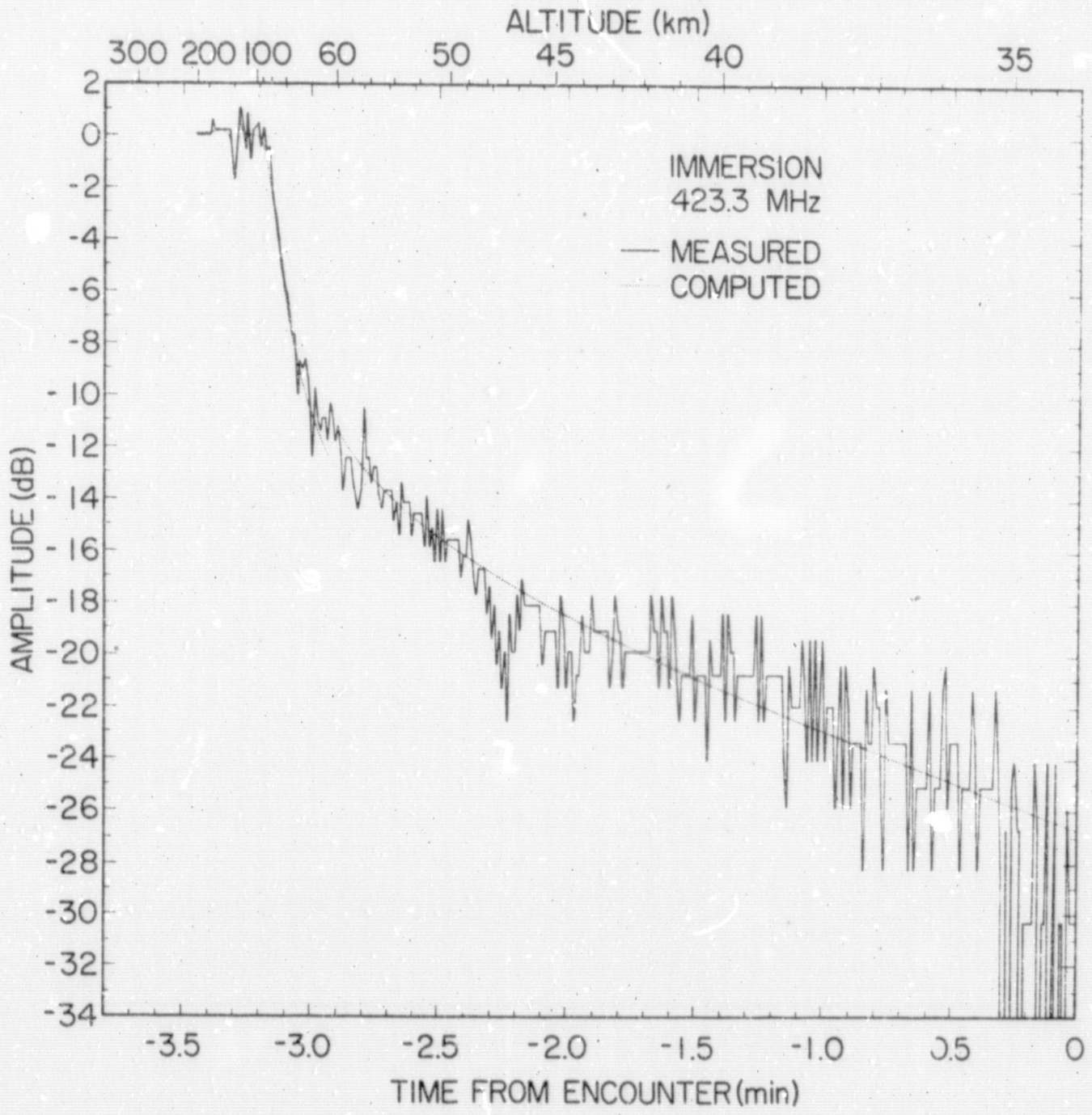

Fig. 9. OBSERVED AND COMPUTED AMPLITUDE VARIATIONS AT 423.3 MHz DURING IMMERSION. Filtered version of amplitude data appeared in the preliminary report [Mariner Stanford Group, 1967].

every 0.6 s. The four amplitude minima observed during the time interval discussed here may have been caused by four thin ionization layers with density on the order of 10^4 el/cm^3. These layers would have to be located very low in the atmosphere, the lowest layer near the 1-mB pressure level at the 87-km altitude (see Fig. 12) and the highest near the 120-km altitude. As discussed below, the amplitude fluctuations may also be scintillation effects caused by horizontal irregularities in the ionization profile near the 142-km altitude level. Such irregularities, or patches, are commonly observed in the terrestrial E region [Smith, Jr., 1957].

Based on ray theory, defocusing produced behind a spherically symmetric ionization blob with gaussian electron density distribution [$N(r) = N_o \exp(-r^2/a^2)$] is given to first order by

$$G_r \approx -700 \sqrt{\pi} \frac{N_o z_s}{f^2 a} \exp(-\rho^2/a^2) \left[1 - \left(\frac{\rho}{a}\right)^2\right] \quad \text{(dB)}$$

where

G_r = focusing behind the blob (dB)
f = radio frequency (Hz)
N_o = electron number density at center of the blob (m^{-3})
a = radius of blob at the $N_o/\exp$ density level (m)
z_s = distance between spacecraft and blob (approximately 10^7 m)
ρ = distance between center of blob and radio ray (m).

Using the above equation, the size and density required can be estimated, if blobs of this type are to explain the observed variations in the 423.3-MHz signal level between -3.26 and -3.18 min from encounter. It is found that a 1-dB dip in the amplitude of 0.5-s duration requires a gaussian ionization patch of 1.8-km radius and a central density of 2.7×10^4 el/cm^3. Note that the defocusing is proportional to the ratio between the density N_o and the radius a. Thus, smaller blobs with lower density would also explain the observations. However, the size and density cannot be determined if the blobs have a radius smaller than 1.8 km because of the limitations imposed by the amplitude sampling rate.

The 423.3-MHz amplitude data do not yield a unique electron number-density distribution. It is believed that the maximum defocusing observed at -3.3 min from encounter should be interpreted in terms of a layer, but the successive fluctuations in the signal level may have been caused by either layers or patches. Further analysis of the S-band doppler measurements might throw new light on the night-side ionosphere of Venus [Kliore et al, 1968].

Figure 10 shows the variations measured in the 49.8-MHz signal level

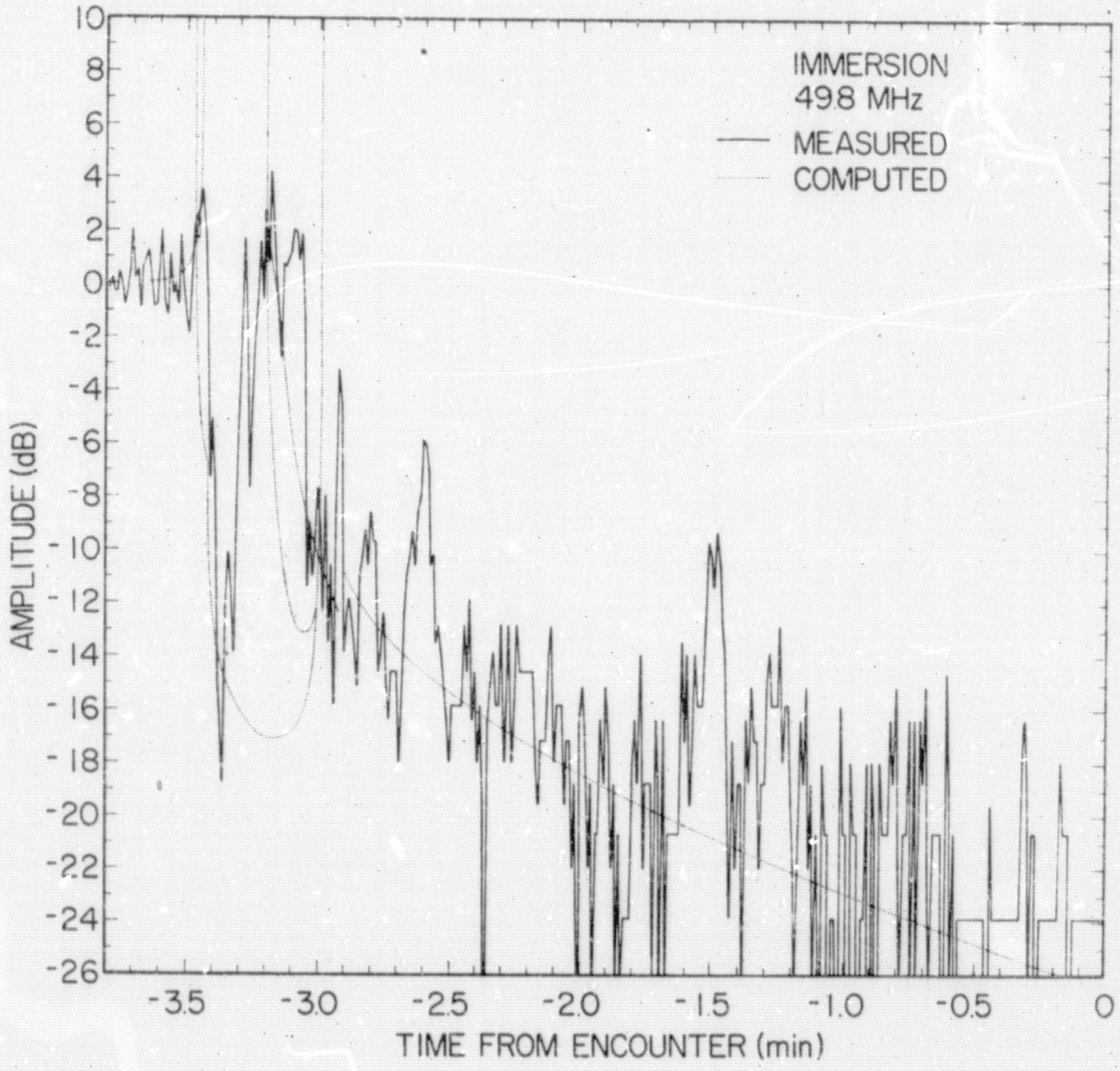

Fig. 10. OBSERVED AND COMPUTED AMPLITUDE VARIATIONS AT 49.8 MHz DURING IMMERSION.

(full-drawn curve) and the amplitude computed from the ionization profile in Fig. 8 (stippled curve). The ionization profile in Fig. 7 yields essentially the same variations in signal level because the high-altitude topside--where it differs from the profile shown in Fig. 8--contributes very little to the focusing.

Computed and observed differential dopplers are shown in Fig. 11. Note in comparing the two curves that frequency splitting caused by multipath propagation cannot be observed with phase-locked receivers, and only data obtained prior to -3.44 min could be utilized in the doppler inversion procedure.

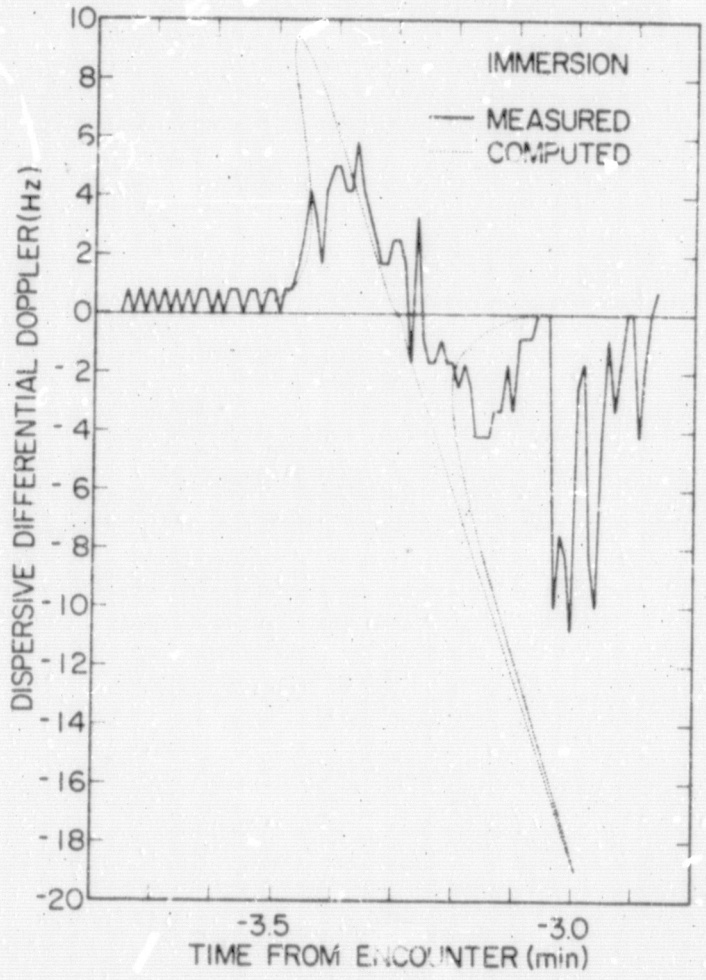

Fig. 11. OBSERVED AND COMPUTED DIFFERENTIAL DOPPLERS VS TIME DURING IMMERSION.

The 49.8-MHz receiver remained locked to the signal coming nearly straight from Earth until it passed through the second caustic at -3.44 min from encounter. It then locked onto a much weaker signal that was defocused by the main layer. From then on, there are large differences between the measured and the computed properties of the 49.8-MHz signal. These differences are probably the result of ionospheric irregularities that cause the signal to arrive at the spacecraft via a large number of different ionospheric paths. Blobs of the type used to explain the 423.3-MHz amplitude fluctuations would produce very large amplitude changes at 49.8 MHz. Some of the deep nulls in the amplitude data may correspond to locations where the receiver changed lock from one ray to another. As discussed previously, there is no method to determine the exact shape and location of these ionospheric inhomogeneities; therefore, they are not included in the calculation of the stippled curves in Figs. 10 and 11.

All amplitude computations illustrated in the figures of this report are based on ray theory. This approach does not provide an accurate representation of the amplitude of signals passing through regions where the structure of the ionosphere is small when compared to the Fresnel zone. A more precise calculation would require wave-theory treatment. The limitations of ray theory are particularly obvious at the caustics, where it predicts infinite signal amplitudes. The wave theory is in much better agreement with observations and yields a finite signal level in these regions. An approximate solution, based on the Huygens-Kirchhoff principle, is available for the caustic regimes [Budden, 1961], and the signal intensity is expressed in terms of tabulated Airy integrals.

The size of the first Fresnel zone is a convenient measure of the altitude resolution that can be achieved by the occultation experiment. In the absence of atmospheric refraction, the diameters of the first Fresnel zone are 5 and 14 km at 423.3 and 49.8 MHz, respectively. Refraction has the effect of changing these zones from circular to elliptic. In the atmospheric and ionospheric regions that produce defocusing, the curvature of the wavefronts is increased in such a way as to squash the Fresnel zones into ellipses with minor axes in the vertical direction. The result is an improved altitude resolution in regions that cause defocusing; conversely, the resolution is reduced in those portions of the ionosphere that produce focusing.

The dual-frequency receiver was originally designed for interplanetary measurements [Koehler, 1965; Long and Fair, 1968]. The Mariner 5 experiment was, therefore, best suited for probing regions with small electron number-density gradients. Multipath propagation in the principal ionospheric layers introduced ambiguities in the differential doppler data; thus, it was necessary to utilize the less accurate amplitude data in studying these regions. One method to improve the differential doppler measurements would be to record the frequency splitting caused by multipath propagation instead of relying entirely on phase-locked receivers. Another method to increase the versatility of these measurements would be to include one or more higher radio frequencies in the experiment [Fjeldbo et al, 1965]. Such measurements are being planned for the Mariner mission to Mars in 1971.

Chapter IV

THE LOWER ATMOSPHERE

Composition measurements made with the USSR lander, Venera 4 [Vinogradov et al, 1968], indicate that CO_2 makes up 90 ± 10 percent of the lower atmosphere of Venus. Molecular nitrogen apparently constitutes less than 7 percent by volume and water vapor 0.1 to 0.7 percent.

None of the gases detected with the Venera 4 instruments would produce a measurable absorption at the radio frequencies employed in the dual-frequency experiment. Thus, it is reasonable to assume that refractive defocusing is the only effect that causes the signal level to decrease behind the atmosphere of Venus. Based on this assumption, one can determine the vertical refractivity profile of the neutral atmosphere probed by the radio signals. This profile, in turn, can be utilized to derive the pressure and temperature profiles of the atmosphere [Fjeldbo and Eshleman, 1968].

Figures 12 and 13 are the vertical pressure and temperature profiles determined by fitting the defocusing produced behind different model atmospheres to the amplitude data obtained during immersion (Fig. 9) and emersion (Fig. 14). Pressure and temperature are seen to differ on the two sides of the planet. To illustrate to what extent the immersion and emersion data differ, Fig. 15 is included to illustrate that the day-side model yields too much defocusing on the night side and the night-side model too little defocusing on the day side.

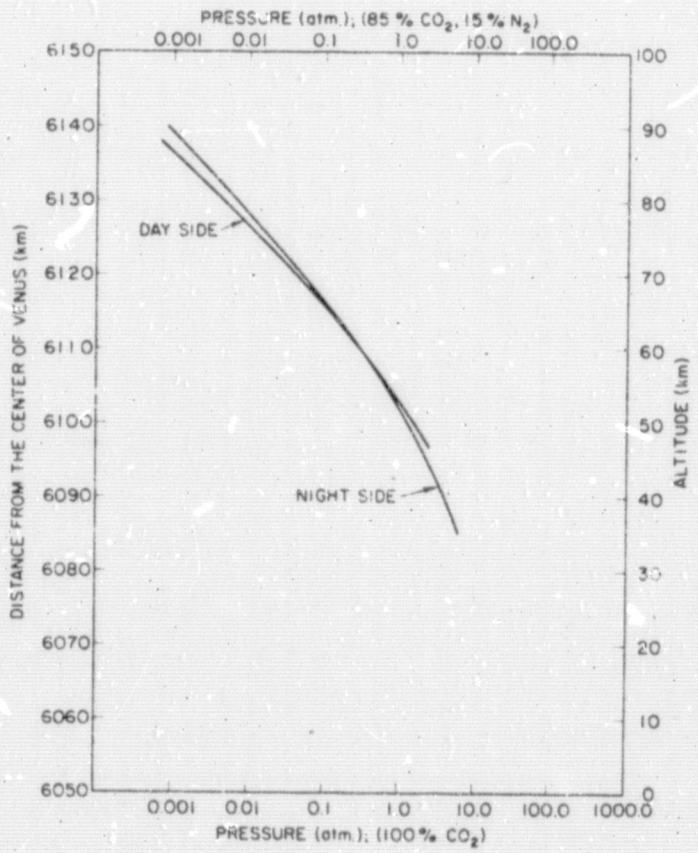

Fig. 12. PRESSURE VS ALTITUDE ON DAY AND NIGHT SIDES OF VENUS.

Preliminary inversion of the S-band doppler data gave essentially the same pressure and temperature profiles on both sides

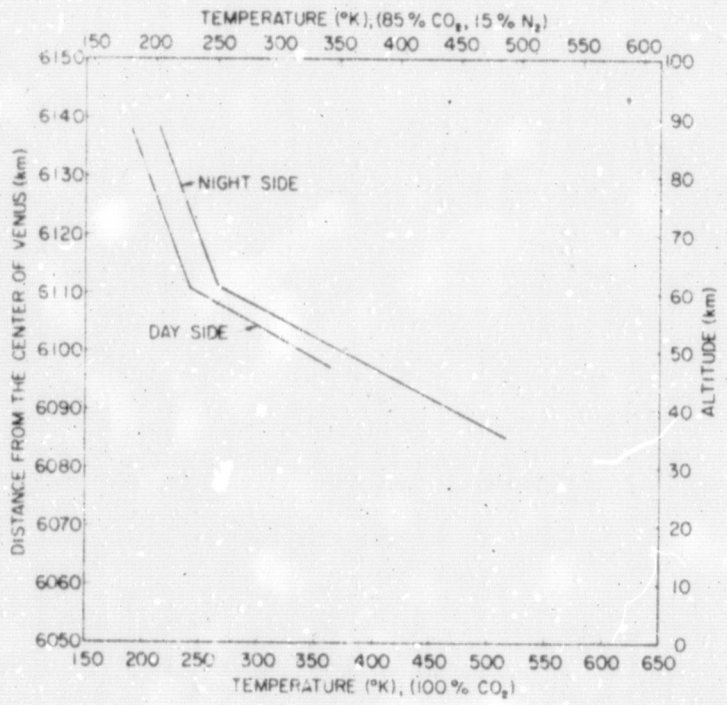

Fig. 13. TEMPERATURE VS ALTITUDE ON DAY AND NIGHT SIDES OF VENUS.

of the planet [Eshleman et al, 1968]. The S-band results are in good agreement with the night-side profiles shown in Figs. 12 and 13 [Kliore et al, 1967; Kliore et al, 1968].

Refraction caused the direction of arrival of the 423.3-MHz signal to change during the occultation experiment, but uncertainties in the spacecraft's antenna gain appear to be too small to account for the differences between the immersion and emersion amplitude data. Variations in transmitter power and receiver amplifier gain were probably also negligible. Absorption in the day-side ionosphere can be ruled out because it is expected to reach a maximum at about 23.0 min from encounter while the propagation path passed tangentially through the lower ionosphere As illustrated by Figs. 14 and 18, any indication of ionospheric absorption does not appear at that time: however, daytime absorption in the neutral atmosphere may have produced the observed amplitude differences. This interpretation would require that the absorbing agent be distributed between the 47 and 60 km altitude in the day-side atmosphere and not be active on the night side of the planet. Ionospheric defocusing, produced by horizontal electron number-density gradients in the day-side ionosphere, also may have contributed significantly to the observed differences.

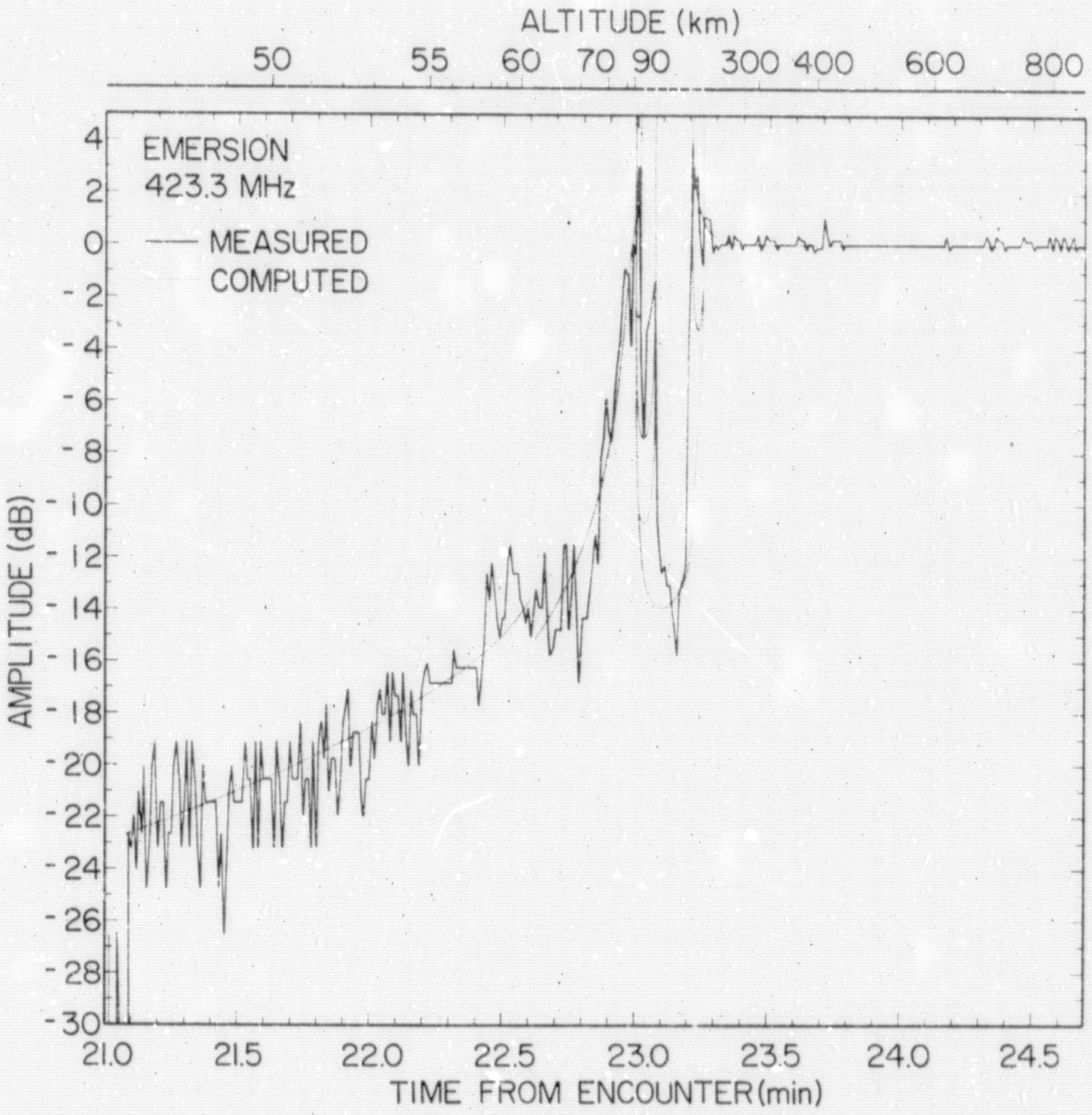

Fig. 14. OBSERVED AND COMPUTED AMPLITUDE VARIATIONS AT 423.3 MHz DURING EMERSION.

The possibility of horizontal ionization gradients in the day-side ionosphere was first noted during the preliminary inversion of the S-band doppler data; this S-band analysis was also based on the assumption of spherical symmetry. It gave a refractivity profile which had a constant

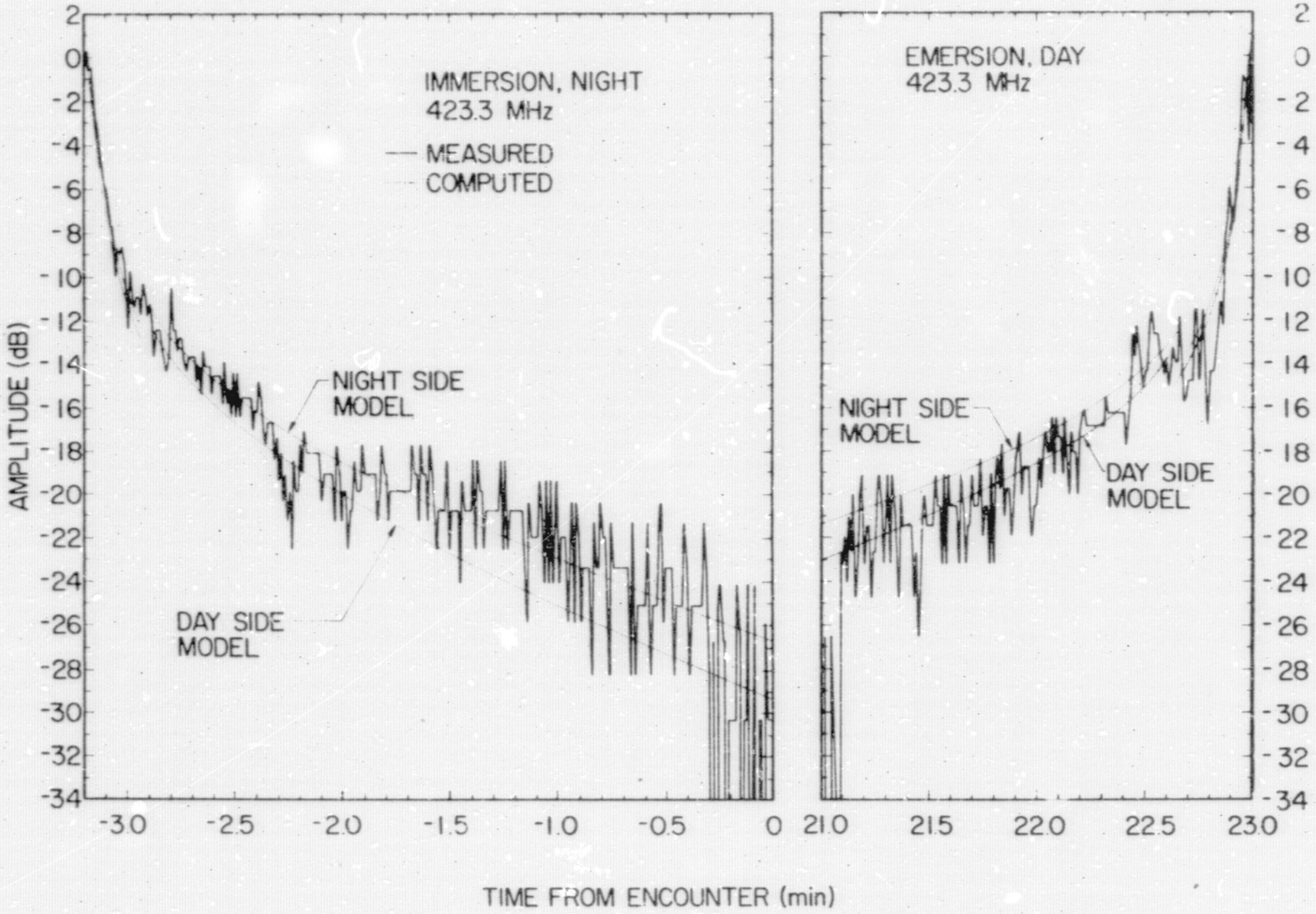

Fig. 15. OBSERVED AND COMPUTED AMPLITUDE VARIATIONS ILLUSTRATING DIFFERENCE BETWEEN DAY- AND NIGHT-SIDE ATMOSPHERES.

positive offset from zero between the neutral atmosphere and the ionosphere. This positive refractivity offset, which occurred in the 100 to 125 km altitude regime where the neutral atmosphere is too thin to measurably affect the radio link, may have been caused by horizontal ionization gradients. However, it is also possible that the offset was produced by frequency drift in the spacecraft's auxiliary oscillator--in this case the S-band temperature profiles would be in error. Further analysis of the S-band amplitude and doppler data and comparison with the results reported here might solve this problem.

Loss of lock on the 423.3-MHz channel occurred at -0.3 min from encounter (see Fig. 9). At this time, the lowest point on the ray passed 35 km above the surface where the pressure was approximately 6 atm. The data do not provide information about the atmosphere below this altitude level. The depth to which the radio ray probed before loss of lock occurred was limited by the transmitter power. However, even with unlimited power, one would not have been able to probe down to the surface because of critical refraction.* The critical-refractive properties of the atmosphere of Venus became known when the USSR lander, Venera 4, made its direct measurements [Avduevsky et al, 1968; Vinogradov et al, 1968] on 18 October 1967 (one day prior to the Mariner 5 occultation experiments).

The spacecraft's dual-frequency instrument continued to sample noise output from the 423.3-MHz amplitude phase detector after loss of lock; data points between -0.3 min and encounter show the relative level of this noise. Signal reacquisition on the 423.3-MHz channel occurred at 21.1 min from encounter, corresponding to an altitude of approximately 47 km. The 49.8-MHz receiver locked up much later because of severe scintillations and critical refraction in the day-side ionosphere (see Fig. 16).

---

*Critical refraction occurs in atmospheric regions where the radius of curvature of a horizontal ray becomes equal to, or smaller than, the distance to the planetary center of mass. No rays can probe tangentially through such regions.

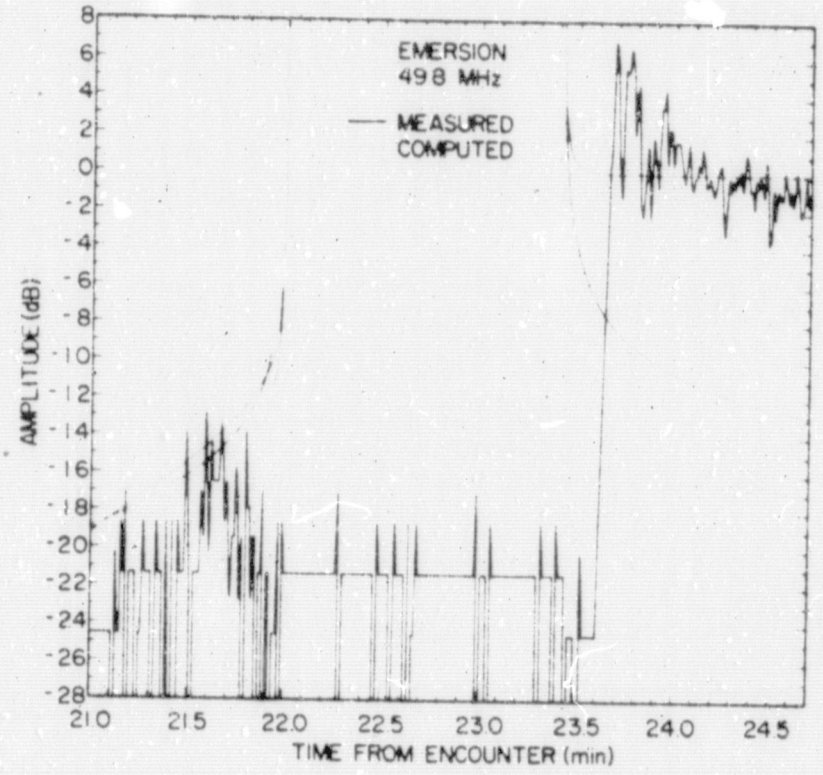

Fig. 16. OBSERVED AND COMPUTED AMPLITUDE VARIATIONS AT 49.8 MHz DURING EMERSION. Amplitude readings below the -20 dB level were produced by instrument noise while the receiver was out of lock.

The discontinuities in the computed amplitude curves at -2.9 and 22.7 min from encounter occurred when the ray grazed the night- and day-side tropopause. The abrupt change in the temperature lapse rate at the tropopause of the model atmosphere produces this effect.

The 423.3-MHz amplitude data show two dips at -2.25 and -2.0 min from encounter; these dips are also present in the S-band data [Kliore et al, 1967], suggesting that they are scintillations caused by refractivity irregularities* or are due to frequency-independent absorption in the neutral atmosphere. Dissipative absorption does not have any effect on the frequency of the signal; however, scintillations would be expected to cause frequency perturbations and perhaps splitting, similar to that shown in Fig. 11. Spectral analysis of the S-band data, therefore, may help to resolve these two possibilities.

---

*A gaussian refractivity blob with a 1-km radius and a temperature of about 10°K above ambient would cause such a dip.

Chapter V

THE DAY-SIDE IONOSPHERE

Inversion of the S-band doppler data provided the day-side ionization profile [Kliore et al, 1968; Kliore et al, 1967]. Caustics were formed behind the main layer at both 49.8 and 423.3 MHz, and this portion of the dual-frequency data is ambiguous. Portions of the 423.3-MHz amplitude data, however, do add credence to the results obtained from the higher frequency.

Figure 17 shows a smooth fit to the ionization profile, deduced from integral inversion of the S-band doppler measurements. Using this profile, the signal amplitudes at the lower frequencies can be readily computed, and the results are illustrated by the stippled curves in Figs. 14, 16, and 18. Figure 18 shows quite clearly how the 423.3-MHz receiver changed lock from one ray to another during emersion--always trying to remain phase locked to the strongest signal available. Note that the computed (stippled) curves do not include the effects of ionospheric and atmospheric irregularities which caused severe scintillations on both radio links.

Calculations of the 49.8-MHz amplitude (see Fig. 16) show the absence of any signal from 22.0 to 23.4 min from encounter; this absence was caused by critical refraction on the bottomside of the ionosphere. The vertical plasma gradients in this region were so great that the radius of curvature of a horizontal ray was smaller than the distance to the planet's center of mass. The 49.8-MHz ray, therefore, was unable to probe tangentially up through this region of the ionosphere.

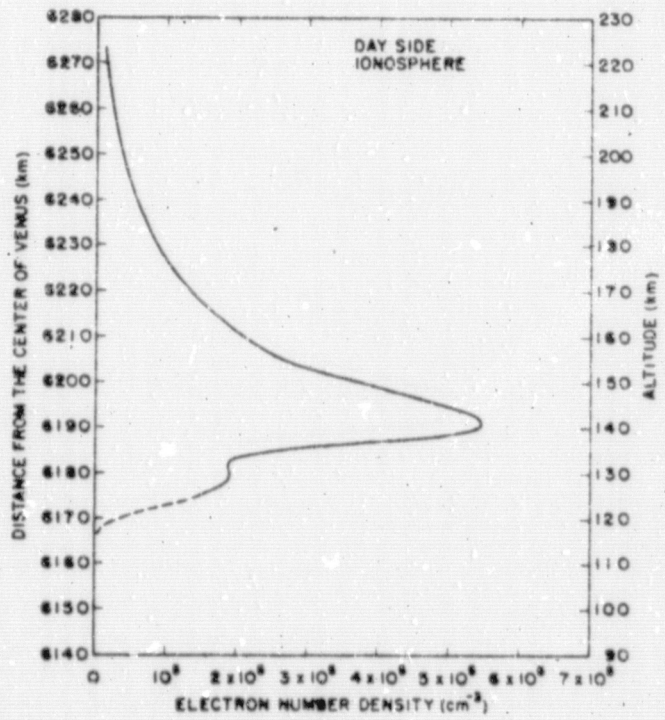

Fig. 17. SMOOTH FIT TO THE DAY-SIDE IONIZATION PROFILE DEDUCED FROM INVERSION OF THE S-BAND DOPPLER MEASUREMENTS.

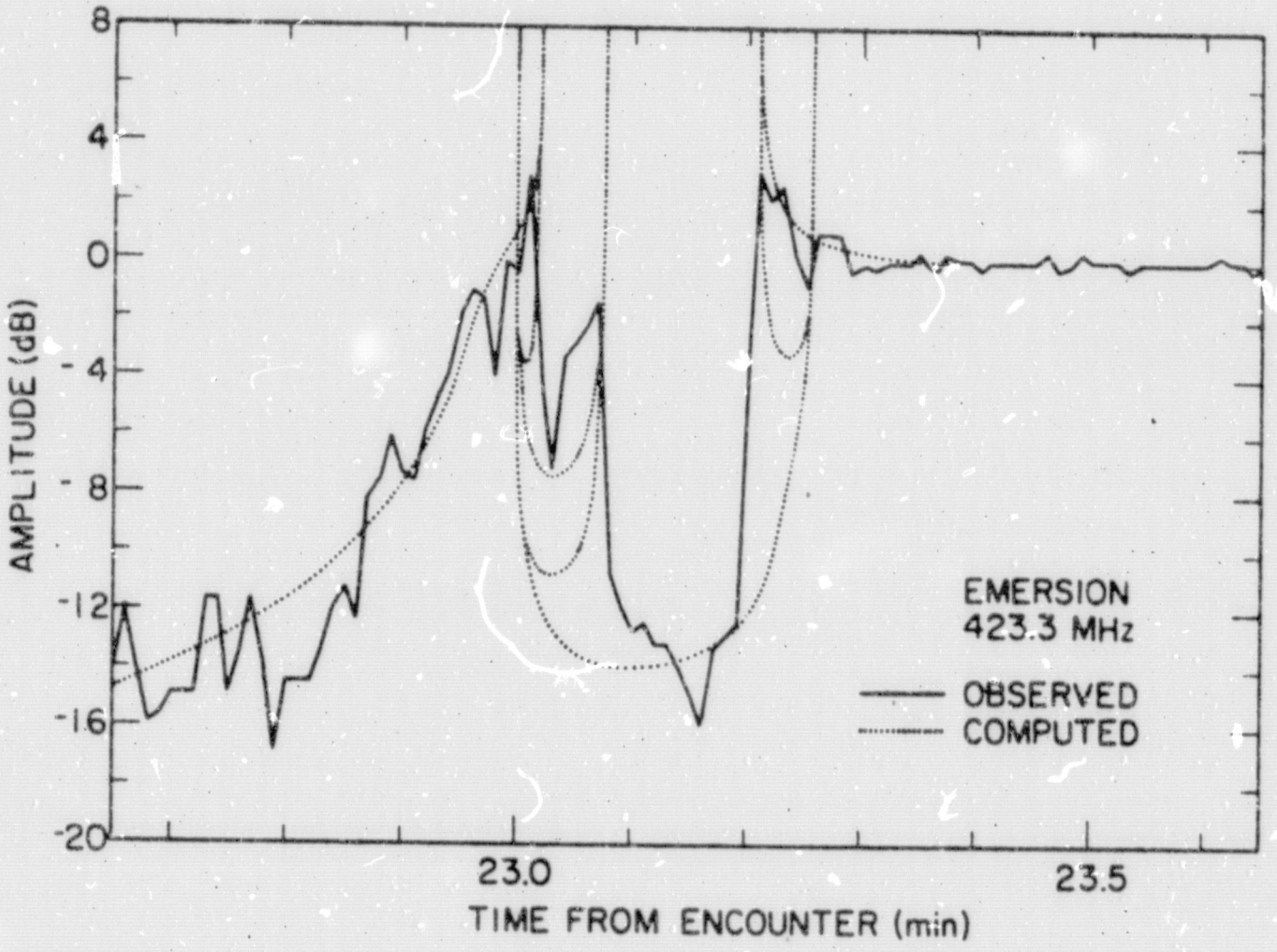

Fig. 18. OBSERVED AND COMPUTED AMPLITUDE VARIATIONS AT 423.3 MHz BEHIND DAY-SIDE IONOSPHERE.

Figure 16 shows two computed signals after 23.4 min from encounter. The strongest signal came directly from Earth; the weaker one was bounced off the ionosphere before arriving at the spacecraft. Prior to 22 min, two signals were also present at the lower frequency, having entered the ionosphere at a sufficiently steep angle of incidence so as to penetrate the main layers.

The 49.8-MHz receiver reacquired the signal at 23.6 min from encounter, 12 s later than the calculated reappearance of the signal. The delay may have been caused by ionospheric scintillations.

The principal day-side ionization peak has been interpreted either as an F_1 or an E region, having a neutral density of 10^{11} or 5×10^{12} cm^{-3}, respectively [Kliore et al, 1968]. Additional information concerning the density of the upper atmosphere of Venus is available from the photometric observations of the occultation of the bright star, Regulus, on 7 July 1959 [de Vaucouleurs and Menzel, 1960]. De Vaucouleurs and Menzel's

original interpretation of the Regulus measurements favors the E-region hypothesis for the day- and night-side ionization peaks [Kliore et al, 1968]; however, a recent re-evaluation of their analysis conducted by Hunten and McElroy (1968) suggests that the optical data is too noisy to be of much use in choosing between the E and F_1 hypotheses.

Chapter VI

THE DAY-SIDE PLASMAPAUSE

The residual electron-content data shown in Fig. 4 suggest that there are important differences between the ionization distribution on the night and day sides of Venus. As discussed in Chapters II and III, the night-side ionization extended out to the 1000-km altitude or more; the day-side ionosphere appears to terminate abruptly near an altitude of about 500 km. Figures 5 and 6 illustrate schematically the differences between the two sides of the planet.

Figure 19 shows the dispersive doppler readings obtained after re-acquisition of the 49.8-MHz signal at 23.6 min from encounter. The many

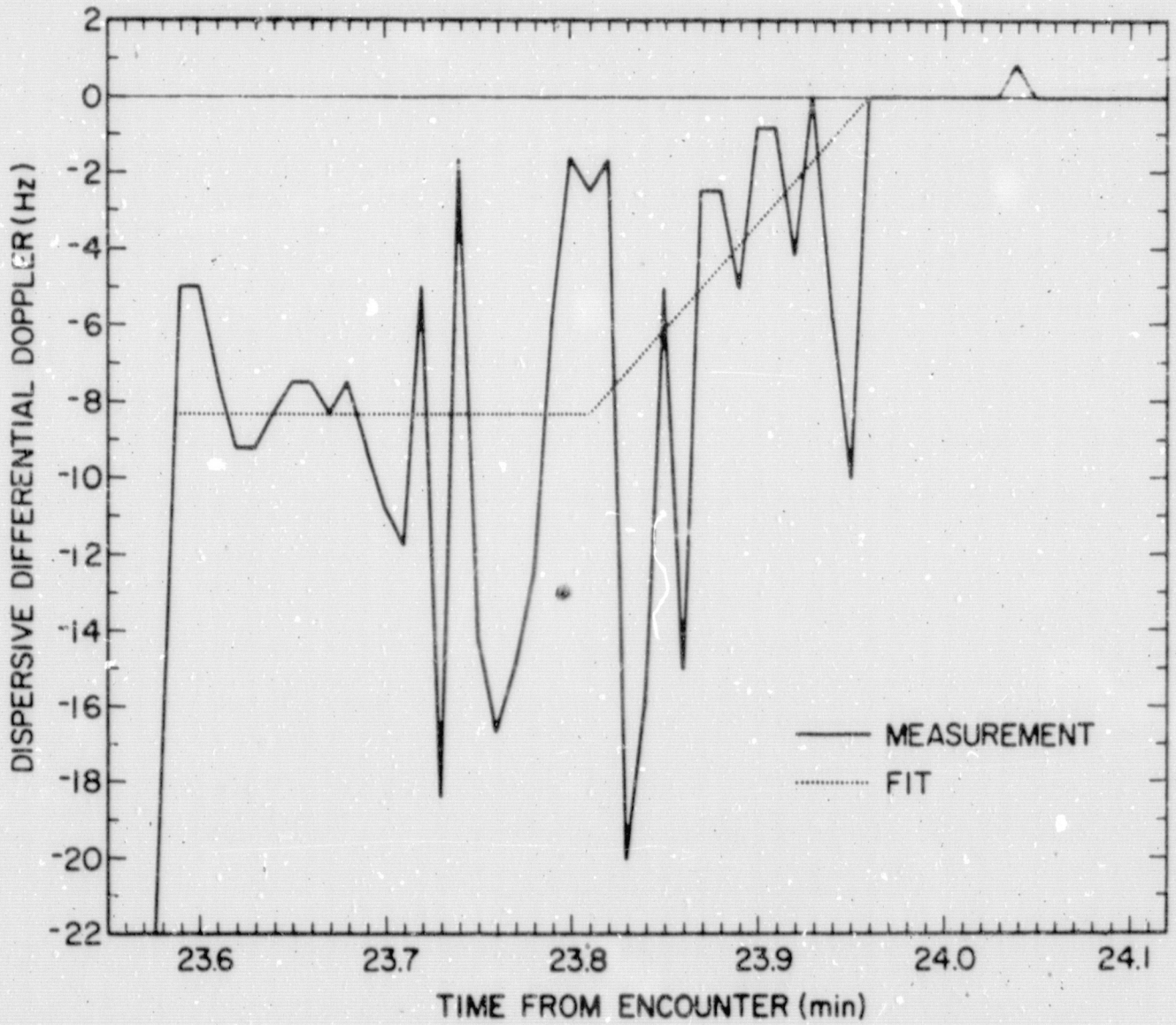

Fig. 19. DISPERSIVE DIFFERENTIAL DOPPLER VS TIME FROM ENCOUNTER. Abrupt termination of dispersive doppler effects at 23.96 min shows that there is no detectable planetary plasma above approximately 520-km altitude.

abrupt doppler changes evident in the data indicate that multipath propagation took place during this period. Some of the doppler counts were undoubtedly made in time intervals when the 49.8-MHz receiver changed lock from one ray to another. These readings are not representative of the actual doppler shifts.

Inversion of the last dip in the doppler data, at 23.95 min from encounter, suggests that this dip corresponds to a 49.8-MHz ray refracted from a ledge of ionization located near the 500-km altitude. This ledge is indicated by the full-drawn curve in Fig. 20. The zero doppler reading, preceding the last dip, corresponds to a ray passing straight through on

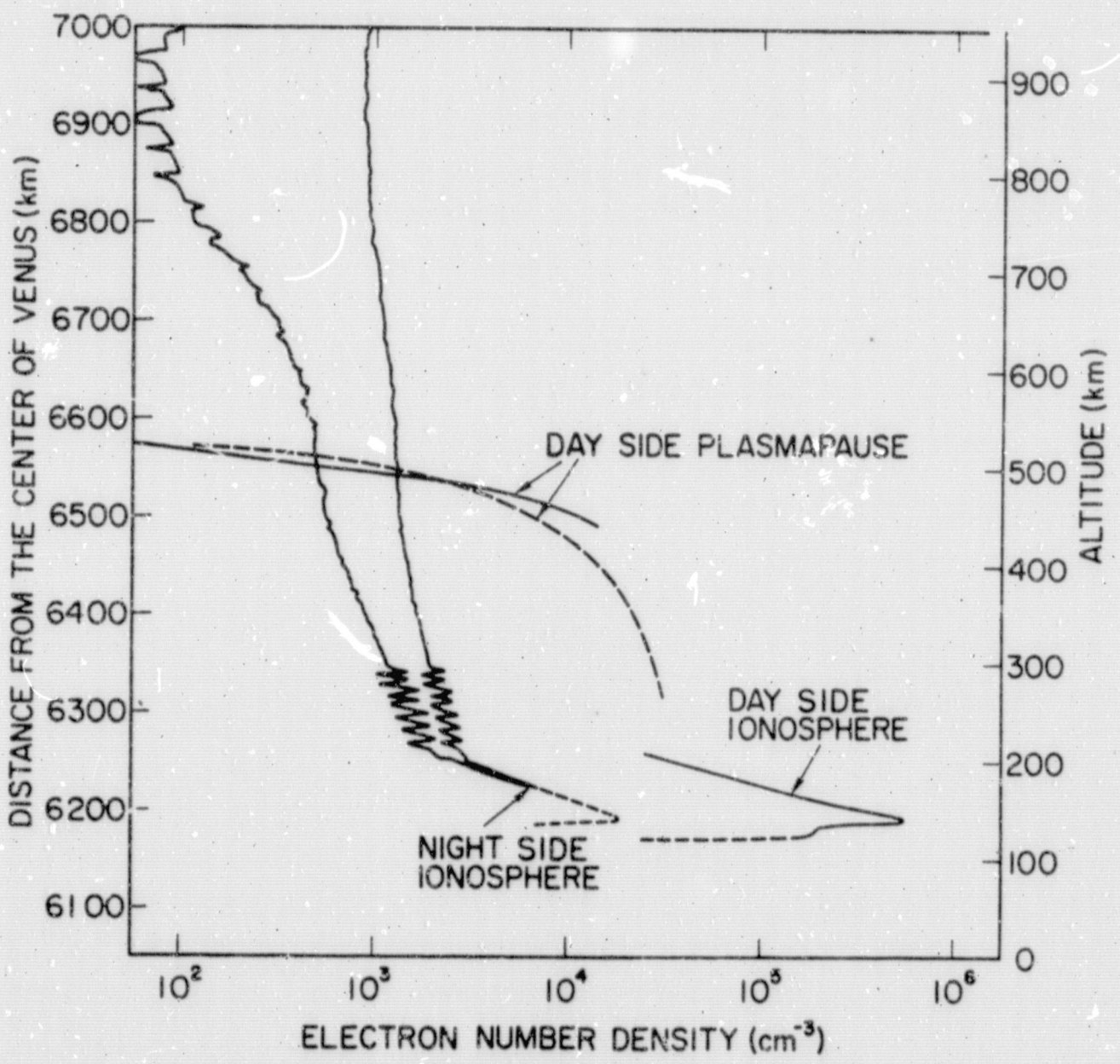

Fig. 20. DAY- AND NIGHT-SIDE IONIZATION PROFILES.

the topside of the ledge. Ray crossovers of this type prevent unambiguous inversion of the raw doppler data. However, a general idea of how the ionization profile should look can be obtained by fitting straight lines to the doppler data, as indicated in Fig. 19; inversion of this fit yields the stippled ionization profile shown between the 250- and 500-km altitude in Fig. 20. Of course detailed resolution is lost by substituting the doppler data with the average straight lines shown in Fig. 19. This procedure may yield the average profile independent of the ionospheric irregularities responsible for the strong fluctuations in the data.

As pointed out in the preliminary report [Mariner Stanford Group, 1967], an unusual amplitude ripple was observed on the 423.3-MHz receiver channel at 23.7 min from encounter (see Fig. 14). This effect probably was caused by an ionospheric irregularity near the 400-km altitude level where the stippled profile of Fig. 20 indicates an electron number density of the order of 1.5×10^4 cm^{-3}.

Neither the amplitude nor the differential doppler data provide information about the ionization distribution between the 200- and 250-km altitude. Further study of the doppler data, obtained from the tracking and telemetry system, may help to bridge this gap.

The day-side plasmapause detected by the dual-frequency experiment probably was produced by the interaction between the conducting ionosphere and the magnetized solar-wind plasma. Venus has little or no intrinsic magnetic field [Bridge et al, 1967; Van Allen et al, 1967], but the planet may be shielded from the solar wind by fields induced by ionospheric currents [Mariner Stanford Group, 1967].

Chapter VII

CONCLUSIONS

The analysis of the Mariner 5 dual frequency occultation measurements has provided a wealth of new information about the atmosphere of Venus but also has brought into focus several unanswered questions. Except for the limitations imposed by critical refraction in the neutral atmosphere, none of these questions must remain unresolved because of fundamental experimental limitations. It is suggested that the implementation of future experiments of this type should emphasize: (1) the resolution of the remaining ambiguities in the day- and night-side plasma distributions on Venus; and (2) the determination of profiles at a large number of local times and positions on Venus.

BIBLIOGRAPHY

Ash, M. E., D. B. Campbell, R. B. Dyce, R. P. Ingalls, R. Jurgens, G. H. Pettengill, I. I. Shapiro, M. A. Slade, and T. W. Thompson, "The Case for the Radar Radius of Venus," Science, 160, May 1968, pp. 985-987.

Avduevsky, V. S., M. Ya. Marov, and M. K. Rozhdestvensky, "Model of the Atmosphere of the Planet Venus Based on Results of Measurements Made by Soviet Automatic Interplanetary Station Venera 4," J. Atmos. Sci., 25, Jul 1968, pp. 537-545.

Barth, C. A., "Interpretation of the Mariner 5 Lyman Alpha Measurements," J. Atmos. Sci., 25, Jul 1968, pp. 564-567.

Bridge, H. S. A. J. Lazarus, C. W. Snyder, E. J. Smith, L. Davis, Jr., and P. J. Coleman, Jr., "Magnetic Fields Observed near Venus," Science, 158, Dec 1967, pp. 1665-1690.

Budden, K. G., Radio Waves in the Ionosphere, Cambridge University Press, Cambridge, England, 1961.

de Vaucouleurs, G. and D. H. Menzel, "Results of the Occultation of Regulus by Venus, July 7, 1959," Nature, 188, 1960, pp. 28-33.

Eshleman, V. R., G. Fjeldbo, J. D. Anderson, A. Kliore, and R. B. Dyce, "Venus: Lower Atmosphere Not Measured," Science, 162, 1968, pp. 661-665.

Fjeldbo, G. and V. R. Eshleman, "The Atmosphere of Mars Analyzed by Integral Inversion of the Mariner 4 Occultation Data," Planetary and Space Sci., 16, 1968, pp. 1035-1059.

Fjeldbo, G., V. R. Eshleman, O. K. Garriott, and F. L. Smith, III., "The Two-Frequency Bistatic Radar Occultation Method for the Study of Planetary Ionospheres," J. Geophys. Res., 70, Aug 1965, pp. 3701-3710.

Goldstein, R. M., "Preliminary Venus Radar Results," J. Res. N.B.S., 69D, 1965, pp. 1623-1625.

Hunten, D. M. and M. B. McElroy, "The Upper Atmosphere of Venus: The Regulus Occultation Reconsidered," J. Geophys. Res., 73, Jul 1968, p. 13.

Kliore, A., D. L. Cain, G. S. Levy, G. Fjeldbo, and S. I. Rasool, "Structure of the Atmosphere of Venus Derived from Mariner 5," Paper No. f.13, presented to the session on the moon and planets, open meeting of W. G. II, 11th COSPAR meeting, Tokyo, Japan, 9-21 May 1968.

Kliore, A., G. S. Levy, D. L. Cain, G. Fjeldbo, and S. I. Rasool, "Atmosphere and Ionosphere of Venus from the Mariner 5 S-Band Radio Occultation Measurement," Science, 158, Dec 1967, pp. 1683-1688.

Koehler, R. L., "A Phase Locked Dual Channel Spacecraft Receiver for Phase and Group Path Measurements," Scientific Report No. 1, Stanford Electronics Laboratories, Stanford University, Stanford, California, Feb 1965.

Long, R. A. and B. C. Fair, "Dual Frequency Receiver System for Mariner 1967 to Venus," Final Engineering Report, SRI Project 5866, Stanford Research Institute, Menlo Park, California, Jun 1968.

Mariner Stanford Group, "Venus: Ionosphere and Atmosphere as Measured by Dual-Frequency Radio Occultation of Mariner 5," Science, 158, Dec 1967, pp. 1678-1683.

McElroy, M. B., "The Upper Atmosphere of Venus," J. Geophys. Res., 73 Mar 1968, pp. 1513-1521.

Melbourne, W. G., D. O. Muhleman, and D. A. O'Handley, "Radar Determination of Radius of Venus," Science, 160, May 1968, pp. 987-989.

Smith, E. K., Jr., "Worldwide Occurrence of Sporadic E," N.B.S. Circular 582, Department of Commerce, Washington, D.C., 15 Mar 1957.

Van Allen, J. A., S. M. Krimgis, L. A. Frank, and T. P. Armstrong, "Venus: An Upper Limit on Intrinsic Magnetic Dipole Moment Based on Absence of a Radiation Belt," Science, 158, Dec 1967, pp. 1673-1675.

Vinogradov, A. P., U. A. Surkov, and C. P. Florensky, "The Chemical Composition of the Venus Atmosphere Based on the Data of the Interplanetary Station Venera 4," J. Atmos. Sci., 25, Jul 1968, pp. 535-536.